

Effect of Metal Ions on Monolayer Collapses

S. Kundu, A. Datta,* and S. Hazra

Surface Physics Division, Saha Institute of Nuclear Physics, 1/AF Bidhannagar,
Kolkata 700064, India

Received March 3, 2005. In Final Form: April 11, 2005

A Langmuir monolayer of stearic acid on pure water and in the presence of certain divalent metal ions such as Cd and Pb at pH \approx 6.5 of the subphase water collapses at constant area, while for other divalent ions such as Mg, Co, Zn, and Mn at the same subphase pH the monolayer collapses nearly at constant pressure. Films of stearic acid with Cd, Pb, Mn, and Co in the subphase (at pH \approx 6.5) have been transferred onto hydrophilic Si(001) using a horizontal deposition technique, just after and long after collapse. Electron density profiles obtained from X-ray reflectivity analysis show that a three-molecular-layer structure starts to form just after constant area collapse, where in the lowest molecular layer, in contact with the substrate, molecules are in asymmetric configuration, i.e., both hydrocarbon tails are on the same side of the metal-bearing headgroup that touches the substrate, while the molecules above the first layer are in symmetric conformation of the tails with respect to the headgroups. Further along collapse, when the surface pressure starts to rise again with a decrease in area, more layers with molecules in the symmetric configuration are added, but the coverage is poor. On the other hand, only bimolecular layers form after constant pressure collapse, with the lower and upper layers having molecules in asymmetric and symmetric configurations, respectively, and the upper molecular layer density increases with compression of the monolayer after collapse. A “Ries mechanism” for constant area collapse and a “folding and sliding mechanism” for constant pressure collapse have been proposed.

Introduction

A Langmuir monolayer is a thermodynamically metastable two-dimensional phase¹ and can show two- to three-dimensional phase transitions under overcompression, where modified structures are formed in the direction perpendicular to the water surface. Such a transition occurs at a particular surface pressure called the collapse pressure (π_c), and the newly formed state is called the collapsed state.² There are two distinct signatures of collapse in the surface pressure (π)-specific molecular area (A) isotherms. One is a strong spike where a sudden drop of pressure occurs after π_c at a fixed value of A of the monolayer. This is the “constant area collapse”. Another is a plateau where pressure is constant after π_c over a certain range of area per molecule. This is the “constant pressure collapse”. Different mechanisms have been proposed for monolayer collapse.

In the “Ries mechanism”³ a trilayer is proposed to form in a monolayer collapse in four successive steps, weakening, folding, bending, and breaking, as observed from electron microscopy of transferred films. Atomic force microscopy images of collapsed films of stearic acid by Birdi and Vu⁴ show the presence of monolayer, bilayer, and trilayer steps. Vollhardt et al.⁵ show the presence of three-dimensional “micrograins” a few nanometers in height. From isotherm and light-scattering microscopy the collapse mechanism of the 2-hydroxytetracosanoic acid monolayer has been studied. Three mechanisms⁶ of

collapse have been observed for that particular monolayer: slow collapse by the nucleation and growth of multilayer islands, formation of giant folds into the subphase, and formation of long multiple folds of small amplitude. The monolayer can also be collapsed by buckling,⁷ where buckled regions can coexist with the flat monolayer formed at the interface and can be reversibly incorporated into the monolayer after expansion. A Langmuir monolayer of arachidic acid in the presence of cadmium ions in subphase water of pH 8.9 and at temperature 5 °C starts to buckle in the third dimension with increasing pressure.⁸ Collapse of the stearic acid monolayer has been studied from phase contrast microscopy and π - A isotherms,^{9,10} where a transition from constant area collapse to constant pressure collapse can occur by changing the pH of the subphase.¹⁰ Monolayers of stearic acid collapse under compression by forming different patterns, depending upon pH and divalent metal ions in the water subphase, as observed by phase contrast microscopy.¹¹

Collapsed films are studied on water and also after they are transferred to some solid substrate by the Langmuir–Blodgett (LB) method,¹² by the inverted Langmuir–Schaefer method (ILS),¹³ and by the method used by Kato et al.¹⁴ From structural modification after collapse a possible mechanism has been proposed, especially for

* To whom correspondence should be addressed. E-mail: alokmay.datta@saha.ac.in.

(1) Petty, M. C. *Langmuir–Blodgett Films: An Introduction*; Cambridge University Press: Cambridge, U.K., 1996.

(2) Gaines, G. L. *Insoluble Monolayers at Liquid–Gas Interfaces*; Interscience: New York, 1966.

(3) Ries, H. E., Jr. *Nature* **1979**, *281*, 287.

(4) Birdi, K. S.; Vu, D. T. *Langmuir* **1994**, *10*, 623.

(5) Vollhardt, D.; Kato, T.; Kawano, M. *J. Phys. Chem.* **1996**, *100*, 4141.

(6) Ybert, C.; Lu, W.; Möller, G.; C. Knobler, M. *J. Phys. Chem. B* **2002**, *106*, 2004.

(7) Lipp, M. M.; Lee, K. Y. C.; Takamoto, D. Y.; Zasadzinski, J. A.; Waring, A. *J. Phys. Rev. Lett.* **1998**, *81*, 1650.

(8) Fradin, C.; Braslau, A.; Luzet, D.; Alba, M.; Gourier, C.; Daillant, J.; Grubel, G.; Vignaud, G.; Legrand, J. F.; Lal, J.; Petit, J. M.; Rieutord, F. *Physica B* **1998**, *248*, 310.

(9) Hattai, E.; Hosoi, H.; Akiyama, H.; Ishil, T.; Mukasa, K. *Eur. Phys. J. B* **1998**, *2*, 347.

(10) Hattai, E.; Nagao, J. *Phys. Rev. E* **2003**, *67*, 041604.

(11) Angelova, A.; Vollhardt, D.; Ionov, R. *J. Phys. Chem.* **1996**, *100*, 10710.

(12) Hattai, E.; Fischer, Th. M. *J. Phys. Chem. B* **2002**, *106*, 589.

(13) Gourier, C.; Knobler, C. M.; Daillant, J.; Chatenay, D. *Langmuir* **2002**, *18*, 9434.

(14) Lee, K. Y. C.; Lipp, M. M.; Takamoto, D. Y.; TerOvanesyan, E.; Zasadzinski, J. A. *Langmuir* **1998**, *14*, 2567.

(15) Kato, T.; Matsumoto, N.; Kawano, M.; Suzuki, N.; Araki, T.; Iriyama, K. *Thin Solid Films* **1994**, *242*, 223.

constant pressure collapse,¹² but a basic and thorough understanding of this spontaneous transition from two to three dimensions is missing. In this Article we seek to look at a particular aspect of monolayer collapse—the influence of metal ions in the subphase. Here out-of-plane structural information on stearic acid monolayers, with Co, Mn, Pb, and Cd ions in the subphase, is extracted before and after collapse. All films are deposited on a hydrophilic Si(001) substrate at different positions of the isotherm by a horizontal deposition technique, which is a modification of the inverted Langmuir–Schaefer technique following Kato et al.¹⁴ This MILS (modified inverted Langmuir–Schaefer) method is simple and can be used very easily with any commercial LB trough. Also the inverted Langmuir–Schaefer method is known to cause minimum disturbance to collapsed monolayers.¹³ X-ray reflectivity analysis of the deposited films gives electron density profiles (EDPs) along the film depth, which help to understand the structural evolution during collapse and the corresponding collapse mechanisms.

Experimental Details and Analysis Technique

Stearic acid molecules (Aldrich, 99.98%) were spread from 150 μL of a 0.5 mg/mL chloroform (Aldrich, 99.98%) solution, in a Langmuir trough (KSV 5000), on Milli-Q water (resistivity 18.2 M Ω cm) at room temperature (24 $^{\circ}\text{C}$) containing different chloride salts of 0.5 mM concentration for each isotherm and collapse measurement. The salts used are cobaltous chloride (CoCl_2 ; Merck, 98%), manganese chloride (MnCl_2 ; Merck, 98%), cadmium chloride (CdCl_2 ; Merck, 98%), lead chloride (PbCl_2 ; Merck, 98%), zinc chloride (ZnCl_2 ; Merck, 98%), and magnesium chloride (MgCl_2 ; Merck, 98%). The pH of subphase water was adjusted by sodium bicarbonate (NaHCO_3 ; Merck, 98%) and was maintained at ~ 6.5 – 6.8 at the time of isotherm measurements and film depositions. Only for lead ions NaHCO_3 was not added to the subphase water. A platinum Wilhelmy plate was used to measure the surface pressure of the stearic acid monolayers. Stearic acid monolayers were compressed with a speed of 2 mm/min at the time of isotherm measurement and film depositions.

Films of stearic acid in the presence of different divalent metal ions were deposited on hydrophilic Si(001) substrates. Silicon substrates were made hydrophilic by keeping them in a mixed solution of ammonium hydroxide (NH_4OH ; Merck, 98%), hydrogen peroxide (H_2O_2 ; Merck 98%), and Milli-Q water (ratio of water, NH_4OH , and H_2O_2 , 2:1:1 by volume) for 5–10 min at 100 $^{\circ}\text{C}$. Hydrophilic silicon substrate was kept horizontally in a homemade L-shaped Teflon substrate holder attached to the clip of the trough dipper. The L-shaped substrate holder can be taken out from water to air with the desired speed. At the time of film deposition in the MILS method, the water surface was properly cleaned, and then the L-shaped substrate holder was immersed into water (containing the divalent salts) so that substrate was kept parallel to and ~ 10 mm below the air–water interface. Stearic acid molecules were then spread on the water surface from the same solution (0.5 mg/mL) with the same amount as was spread at the time of isotherm measurement. Depositions were done before, after and far after the collapse pressure. The upward speed of the substrate holder was 0.5 mm/min for all depositions to cause minimum disturbance. We have deposited films in the presence of two metal ions from each group, Cd and Pb for constant area collapse and Mn and Co for constant pressure collapse.

X-ray reflectivity studies of all the deposited films were carried out using an 18 kW rotating anode generator (Enraf Nonius, FR591).¹⁵ The X-ray beam was monochromatized using the (111) face of a silicon crystal, and the radiation was collimated by slits having apertures of 100 and 5000 μm in and perpendicular to the scattering plane, respectively, to define the beam size and geometry as well as to select the $\text{Cu K}\alpha_1$ component (wavelength $\lambda = 1.540562$ \AA). The sample was mounted on the θ arm, and the scattered beam taken through an evacuated path was detected

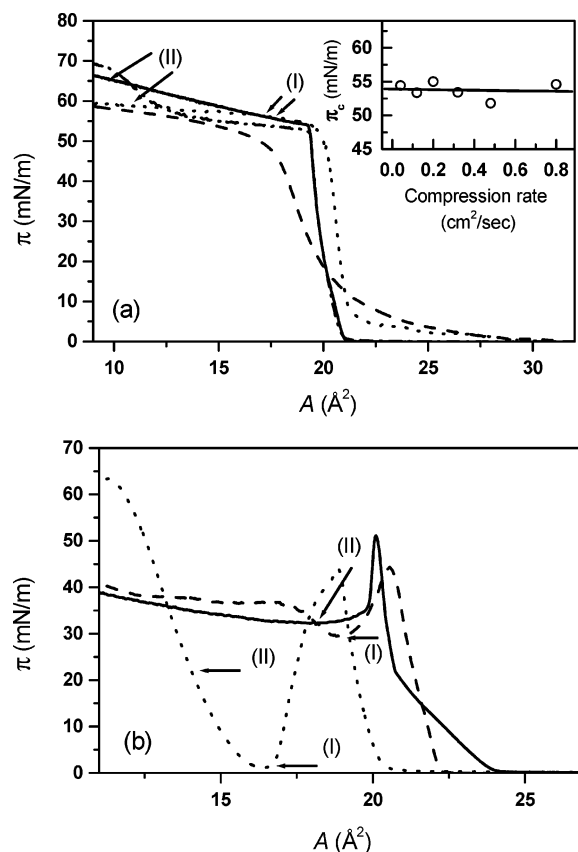


Figure 1. (a) Surface pressure (π)–specific molecular area (A) isotherms of a stearic acid monolayer in the presence of Mn (solid line), Co (dotted line), Zn (dashed line), and Mg (dash-dotted line) ions in subphase water. Inset: collapse pressure (π_c) versus compression rate in the presence of Co ions in subphase water. (b) π – A isotherms of a stearic acid monolayer on pure water (solid line), in the presence of Cd (dotted line) and Pb (dashed line) ions in subphase water. The concentration of each metal ion is 5×10^{-4} M, and the subphase pH ≈ 6.5 . Arrows indicate the points at which films are deposited by the MILS method. Two films at positions I and II are deposited in each case.

by the NaI scintillation detector mounted on the 2θ arm of the goniometer. The sample arm was scanned in steps of millidegrees. Instrumental resolution in the out-of-plane direction was 0.0014 \AA^{-1} . The scattering plane is perpendicular to the sample face. Data were taken in the specular condition; i.e., the incident angle is equal to the exit angle, and both are in the scattering plane. Under specular conditions the momentum transfer vector $\mathbf{q} = \mathbf{k}_f - \mathbf{k}_i$ ($\mathbf{k}_{i(f)}$ = incident (scattered) wave vector) has only one nonvanishing component, q_z , normal to the surface given by $q_z = (4\pi/\lambda) \sin \theta$, where θ is the angle the incident X-ray beam makes with the surface. X-ray reflectivity data of all the films were taken, and analysis was done by the Parratt formalism¹⁶ introducing the finite interfacial width.¹⁷

Constant Pressure Collapse

In the presence of Co, Mn, Mg, and Zn ions in the subphase and at the same pH value (~ 6.5), stearic acid monolayers show constant pressure collapse as depicted in Figure 1a, where a nearly flat pressure region is observed after the corresponding π_c . It was observed that, unlike pure fatty acid monolayers,¹⁸ π_c is invariant with

(16) Parratt, L. G. *Phys. Rev.* **1954**, *95*, 359.

(17) Dailant, J.; Gibaud, A. *X-Ray and Neutron Reflectivity: Principles and Applications*; Springer: Berlin, 1999. Tolani, M. *X-Ray Scattering from Soft Matter Thin Films*; Springer: Berlin, 1999.

(18) Kato, T. *Langmuir* **1990**, *6*, 870. Kato, T.; Hirobe, Y.; Kato, M. *Langmuir* **1991**, *7*, 2208.

compression rate in the presence of Co ions, as shown in the inset of Figure 1a. This shows, probably for the first time, that fatty acid monolayer collapse becomes less of a kinematic process in the presence of metal–headgroup interaction. The isotherms exhibit considerable variation at collapse. While Co and (more so) Zn produce a continuous change in compressibility of the monolayer, resulting in a more “rounded” edge at the collapse point, Mg ions and, in particular, Mn ions cause a discontinuous change in the gradient of the π – A curve, and the collapse point is almost a cusp. Collapse is generally visualized as a combination of formation of 3D nucleation centers and growth merging of these centers¹⁹ and also can be compared to plastic deformation in solids,²⁰ where these nucleation centers are the “defects”. It is interesting to note that the collapse behavior of the monolayer with Mg and Mn ions has a striking similarity with the plastic deformation of ideal crystals, with almost no defects below the critical stress and an occurrence of many defects simultaneously at this stress value.²¹ On the other hand, if there is a small but progressively growing number of defects from a point quite below the critical stress, the plastic deformation curve looks almost exactly like the collapse isotherm with Co and Zn ions. The collapse behaviors in these two sets thus suggest progressive growth of centers for the “continuous change” and simultaneous growth of centers for the “discontinuous change” group.

This difference in the collapse behavior of stearic acid monolayers caused by different metal ions prompted us to deposit and study films collapsed in the presence of a member from each of the above two sets. We chose Co ions from the “continuous” group and Mn ions from the “discontinuous” group. We did not deposit any films before collapse since the structure of Langmuir monolayers with different divalent metal ions in the subphase is well-known.²² Films were deposited by the MILS method just after and far after collapse pressures, and arrows in the isotherms indicate the corresponding points of deposition. Analysis of X-ray reflectivity data collected on these monolayers just before collapse points to a near-perfect monolayer with Mn ions but a highly distorted monolayer with Co ions. These results are consistent with our foregoing conjecture of a sudden growth of 3D centers or defects for the former and a progressive growth from $\pi < \pi_c$ for the latter.

Mn. In the presence of Mn ions in the subphase, monolayer collapse starts at 53.91 mN/m surface pressure (Figure 1a). The pressure after collapse then slowly increases with compression. Figure 2a summarizes the evolution of reflectivity profiles of the stearic acid film with collapse, where I and II correspond to the film just after and far after collapse. Profiles and corresponding best fits based on the Parratt formalism are shifted upward for visual clarity. One of the most important features of the reflectivity profiles is the presence of Kiessig fringes or interference fringes due to the total film, indicating coherence between the air/film and film/substrate interfaces. The other interesting feature is the first strong split peak ($q_z \approx 0.22 \text{ \AA}^{-1}$) that signifies a structure more complex than a single monolayer. Figure 2b shows the corresponding EDPs extracted from the fits. The same protocol

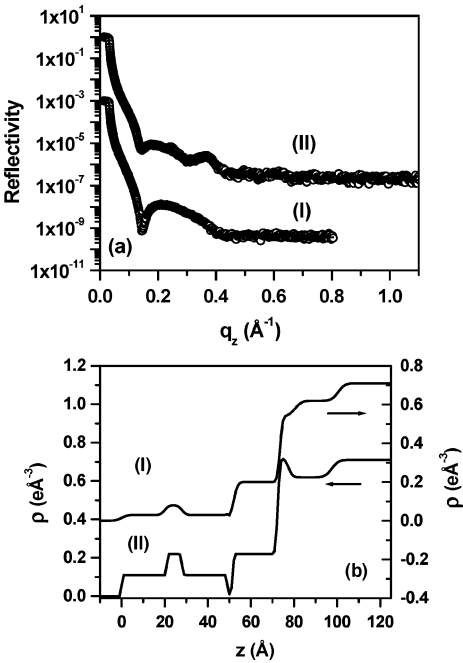


Figure 2. (a) X-ray reflectivity profiles (circles) and corresponding fitted curves (solid line) of the films of stearic acid in the presence of Mn ions in subphase water deposited (I) just after collapse and (II) far after collapse. In this and three other figures, reflectivity profiles have been shifted vertically for clarity. (b) Electron density profiles, i.e., average electron density (ρ) versus depth (z) extracted from the fit of reflectivity profiles I and II. Air is at $z = 0$.

Table 1. Layer Parameters of Films Deposited Just after Collapse (Region I of Collapse) (Obtained from Reflectivity Analysis) Where t Is Thickness (\AA), σ Is Roughness (\AA), and ρ Is Electron Density (e \AA^{-3})

molecular layer parameters			Mn	Co	Cd	Pb
third layer	tail	σ_2	2.00	2.50	1.00	1.00
		ρ			0.04	0.03
		t			22.0	15.0
	head	ρ			0.16	0.07
		t			4.00	7.50
		ρ			0.05	0.03
second layer	tail	t			22.0	15.0
		ρ	0.03	0.03	0.18	0.16
		t	20.0	21.0	21.5	22.0
	head	ρ	0.08	0.08	0.75	0.42
		t	8.00	8.00	5.00	6.50
		ρ	0.03	0.03	0.20	0.16
first layer	tail	t	21.5	21.5	21.5	22.0
		ρ	0.20	0.24	0.25	0.32
		t	21.5	21.5	8.00	8.00
	head	ρ	0.54	0.58	0.55	0.55
		t	7.00	6.50	18.0	13.0
		σ_1	2.50	2.50	4.00	2.00

is followed for all metal ions. Just after collapse (I) it is clear that a bimolecular film has started to form. The molecules in the lower monolayer have a $\sim 7 \text{ \AA}$ thick high-density region (electron density $\sim 0.54 \text{ e \AA}^{-3}$) near the substrate as seen in Table 1. This region corresponds to Mn-containing headgroups. Away from the substrate there is a $\sim 22 \text{ \AA}$ thick lower density (electron density $\sim 0.24 \text{ e \AA}^{-3}$) layer corresponding to the hydrocarbon tails. Thus, hydrocarbon tails are in asymmetric configuration with respect to the metal-bearing headgroup in this monomolecular layer, with two tails in the same direction, away from the substrate. Assuming the density of close-packed hydrocarbon tails to be $\sim 0.32 \text{ e \AA}^{-3}$,¹⁷ the molecular coverage in this lower layer is $\sim 62.5\%$. The upper molecular layer has tails symmetric with respect to the

(19) Vollhardt, D.; Retter, U. *J. Phys. Chem.* **1991**, *95*, 3723.
(20) Kampf, J. P.; Frank, C. W.; Malmström, E. E.; Hawker, C. J. *Science* **1999**, *283*, 1730.
(21) Kovács, I.; Zsoldos, L. *Dislocations and Plastic Deformation*; Pergamon Press: Oxford, U.K., 1973.
(22) Kmetko, J.; Datta, A.; Evmenenko, G.; Dutta, P. *J. Phys. Chem. B* **2001**, *105*, 10818.

Table 2. Layer Parameters of Films Deposited Far after Collapse (Region II of Collapse) (Obtained from Reflectivity Analysis) Where t Is Thickness (Å), σ Is Roughness (Å), and ρ Is Electron Density ($\text{e} \cdot \text{\AA}^{-3}$)

molecular layer parameters			Mn	Co	Cd	Pb
fifth layer	tail	σ_2	0.20	2.50	0.50	0.20
		ρ			0.05	0.04
		t			22.0	21.5
	head	ρ			0.21	0.10
		t			4.00	4.00
		ρ			0.05	0.04
fourth layer	tail	t			22.0	21.5
		ρ			0.10	0.06
		t			22.0	22.0
	head	ρ			0.43	0.22
		t			4.00	4.00
		ρ			0.10	0.06
third layer	tail	t			22.0	22.0
		ρ			0.18	0.10
		t			22.0	22.0
	head	ρ			0.71	0.42
		t			4.00	4.00
		ρ			0.18	0.10
second layer	tail	t			22.0	22.0
		ρ	0.11	0.12	0.18	0.15
		t	21.0	20.0	22.0	22.0
	head	ρ	0.22	0.20	0.71	0.48
		t	7.00	7.00	4.00	4.00
		ρ	0.11	0.13	0.18	0.15
first layer	tail	t	21.0	21.0	22.0	22.0
		ρ	0.22	0.20	0.22	0.21
		t	21.0	21.0	15.5	6.00
	head	ρ	0.72	0.55	0.40	0.54
		t	5.00	7.00	12.5	15.5
		σ_1	1.50	2.50	5.00	3.65

headgroups; i.e., two tails are in the two sides of the headgroups with a molecular coverage of $\sim 9.4\%$. This combination of asymmetric and symmetric molecular configurations has been observed in LB films of deposited fatty acid in the presence of divalent metal ions.²³ Far after collapse (II), again only a bimolecular layer model fits the data, where the molecular coverages in the lower and upper monomolecular layers (Table 2) are $\sim 68.75\%$ and $\sim 34.4\%$, respectively. We also observe that the headgroup has become thinner and denser in the lower layer in region II with respect to region I and both interfacial widths have decreased, reflecting better packing in this region of collapse.

Co. In the presence of Co ions in the subphase water the stearic acid monolayer collapses at 54.0 mN/m surface pressure (Figure 1a), and then the pressure remains nearly constant with compression. Figure 3a shows the evolution of reflectivity profiles and corresponding fit of the stearic acid film with collapse, where I and II correspond to the film just after and far after collapse. The reflectivity profiles are almost identical in their features to those obtained with Mn ions. In Figure 3b, corresponding EDPs are shown extracted from fitting. Just after collapse (I) it is clear from EDP that a bimolecular layer has started to form. Tables 1 and 2 show the surprising similarity with the case of Mn ions. Not only the conformations of molecules in the two layers but also the thickness and density of each sublayer are very similar for both regions I and II. The upper monomolecular layer has $\sim 9.4\%$ coverage, the same as obtained with Mn ions. But the coverage in the lower monolayer is more ($\sim 75\%$) than the coverage of the corresponding layer in region I for Mn ions, indicating a more compact film being caused by Co

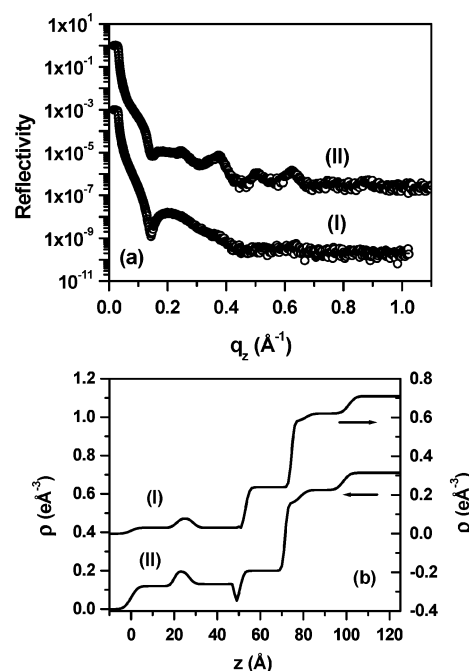


Figure 3. (a) X-ray reflectivity profiles (circles) and corresponding fitted curves (solid line) of the films of stearic acid in the presence of Co ions in subphase water deposited (I) just after collapse and (II) far after collapse. (b) Average electron density (ρ) versus depth (z) extracted from the fit of reflectivity profiles I and II.

ions. Further along collapse in region II, the molecular coverages are $\sim 41\%$ and $\sim 62.5\%$ in the upper and lower monolayers, respectively, suggesting transfer of molecules from the lower to upper layer. With Mn ions, the molecular coverages increase in both the upper and lower layers from region I to region II; hence, transfer of molecules from the lower to upper layer is less apparent.

Thus, out-of-plane molecular layer information obtained from X-ray reflectivity analysis of collapsed films of fatty acid in the presence of two metal ions at constant surface pressure shows that a bimolecular layer is formed after collapse and such a layered structure is maintained with compression, the upper layer coverage increasing with compression. This behavior is invariant with the behavior of the monolayer at the collapse point, i.e., whether it is continuous or discontinuous collapse, as long as it is a constant pressure collapse. This is summarized in Figure 6a,b. The constancy of height during constant pressure collapse is consistent with cylindrical nucleation centers rather than with the hemispherical centers proposed by Vollhardt and Retter.¹⁹ The constancy of the bimolecular structure at constant pressure collapse can be consistent with the Ries mechanism³ only if the folded and weakened monolayer formed during collapse bends and falls always on another monolayer region. In the collapsing monolayer there is nothing to drive the monolayer to such a preferential deposition. On the other hand, the continued folding-and-sliding mechanism proposed by Gourier et al.,^{12,24} where collapse happens by folding of the monolayer and then sliding of the folded monolayer over the rest of the monolayer, is quite consistent with our observation of a continuously condensing bimolecular layer during constant pressure collapse.

Constant Area Collapse

Constant area collapse is observed for a stearic acid monolayer on pure water in the π -A isotherm. A stearic

(23) Malik, A.; Durbin, M. K.; Richter, A. G.; Huang, K. G.; Dutta, P. *Phys. Rev. B* **1995**, 52, R11654. Englisch, U.; Penacorada, F.; Samoilenko, I.; Pietsch, U. *Physica B* **1998**, 248, 258.

(24) Nikomarov, E. S. *Langmuir* **1990**, 6, 410.

acid monolayer collapses at 51 mN/m surface pressure and at 20.1 Å² area per molecule. The same types of constant area collapse are also observed for a stearic acid monolayer in the presence of cadmium and lead ions in subphase water, which is shown in Figure 1b. In all cases, the monolayer shows a sudden drop in surface pressure at constant A just after π_c . This sudden drop in surface pressure indicates²⁵ the growth of 3D nucleation centers at a much faster rate than the compression of the monolayer, leading to a reduction in the monolayer surface density. The monolayer can respond to this fast reduction by either rapidly restructuring to a different, i.e., low-pressure phase or by forming “cracks” or “voids”, i.e., patches of bare water surface within the film. Then, after passing through this region of low pressure, the film again shows a rise of π with a decrease in A . However, there are significant differences among the three cases. The monolayer in the presence of Cd ions shows the biggest fall in π (~ 42 mN/m), whereas the monolayer with Pb ions shows the smallest fall (~ 14 mN/m) though π_c is almost the same (~ 44 mN/m) for both. Monolayers in the presence of metal ions show a slower fall compared to the pristine monolayer. But the monolayer in the presence of Pb ions has collapse features that are quite similar to those of the pristine monolayer, in contrast to the collapse behavior in the presence of Cd ions. Since subphase pH has not been altered with any external agents for the pristine monolayer and the monolayer with Pb ions, the difference in the Cd ion case may be attributed to the effect of subphase pH. Here, in particular, the monolayer has collapsed to $\pi \approx 0$ mN/m, a value very difficult to reconcile with restructuring of the monolayer. Collapsed films were transferred onto silicon substrates at positions I and II indicated by arrows in Figure 1b, where I is in the low-pressure region and II is in the second region of rise of π with a decrease in A .

Cd. In Figure 4a reflectivity profiles of stearic acid films and corresponding fits are shown which are deposited in the low-pressure region (I) and the region of rising pressure (II) indicated in the isotherm of Figure 1b. The reflectivity profiles show a clear discontinuity between these regions. Whereas in region I there are broad, weak Bragg peaks indicating few molecular layers, region II is dominated by a number of strong, sharp Bragg peaks, which are a signature of a multilayer structure. The extracted EDPs are shown in Figure 4b. It is clear from the EDP that in region I three monomolecular layers have been deposited on a silicon substrate, where the coverage decreases from $\sim 78.2\%$ to $\sim 62.5\%$ and then to $\sim 12.5\%$ from bottom to top. As shown in Table 1 for region I, the first monolayer in contact with the substrate has molecules in the asymmetric configuration with respect to the metal-bearing headgroup, with anomalous headgroup and tail thickness. We attribute the increase in headgroup thickness to cadmium oxide or hydroxide formation on the substrate and the decrease in tail thickness to a tilt with respect to vertical. The molecules in the upper two monolayers are in symmetric configuration with respect to the headgroups. In other words, the film in region I of monolayer collapse in the presence of Cd ions has a strong resemblance to the first three layers of a growing LB film.²⁶ In region II of collapse the EDP indicates formation of a multilayer consisting of five molecular layers with a progressively decreasing coverage after the third monolayer. The coverages from the bottom to top molecular

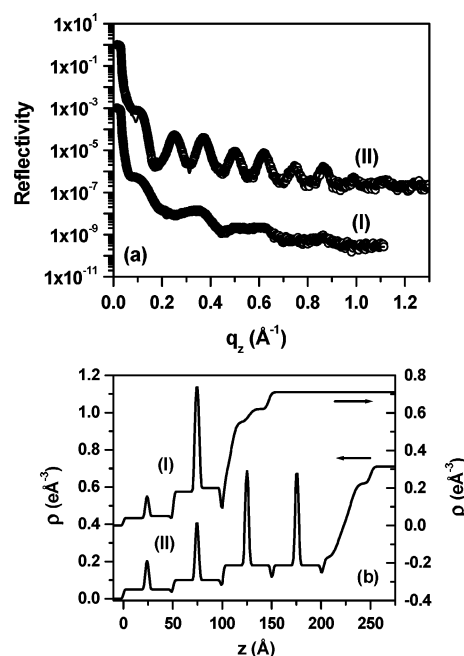


Figure 4. (a) X-ray reflectivity profiles (circles) and corresponding fitted curves (solid line) of the films of stearic acid in the presence of Cd ions in subphase water deposited (I) just after collapse and (II) far after collapse. (b) Average electron density (ρ) versus depth (z) extracted from the fit of reflectivity profiles I and II.

layers are $\sim 68.75\%$, $\sim 56.25\%$, $\sim 56.25\%$, $\sim 31.25\%$, and $\sim 15.6\%$, respectively. The decrease of molecules from the bottom layer may be due to transfer to the upper layers from region I to region II. The first layer (Table 2) has molecules in the asymmetric configuration, whereas the rest of the layers have molecules in symmetric configuration with respect to the metal-bearing headgroups. Hence, in this second region of constant area collapse a multilayer structure with progressively decreasing coverage is formed on the water surface as evidenced by the presence of the positive surface pressure of the film on the water surface, which increases with a decrease in the specific molecular area, and also directly from the transferred film structure.

Pb. For Pb ions in subphase water the stearic acid monolayer collapse starts at 44 mN/m surface pressure (Figure 1b). In Figure 5a reflectivity profiles and the corresponding fits are shown for the films, which correspond to region I and region II as shown in Figure 1b and also to regions I and II of the Cd ion case. The reflectivity profiles are also similar to those obtained for Cd ions. The EDPs shown in Figure 5b, which have been extracted from the fits of the data in Figure 5a, also are very similar to those of a monolayer collapsed with Cd ions in the subphase. Table 1 confirms that, as with Cd ions, the collapsed monolayer at region I forms a trimolecular layer in the same molecular configuration as with Cd ions and with coverages of $\geq 95\%$, $\sim 50\%$, and 9.4% in the three layers from bottom to top. Table 2 shows that, after this, in an apparently discontinuous process, a multilayer with a gradually depleting coverage of $\sim 66\%$, $\sim 46.8\%$, $\sim 31.25\%$, $\sim 18.75\%$, and $\sim 12.5\%$ from bottom to top is formed. A transfer of molecules from bottom to top during passage from region I to region II is again observed. The situation for constant area collapse is depicted by Figure 6c,d. The formation of such multilayers through random deposition of two to four layers of molecules in the symmetric configuration on a monolayer of molecules in the asymmetric configuration is consistent with the

(25) Saville, P. M.; White, J. W.; Hawker, C. J.; Wooley, K. L.; Fréchet, J. M. J. *J. Phys. Chem.* **1993**, *97*, 293.

(26) Sanyal, M. K.; Mukhopadhyay, M. K.; Mukherjee, M.; Datta, A.; Basu, J. K.; Penfold, J. *Phys. Rev. B* **2002**, *65*, 033409.

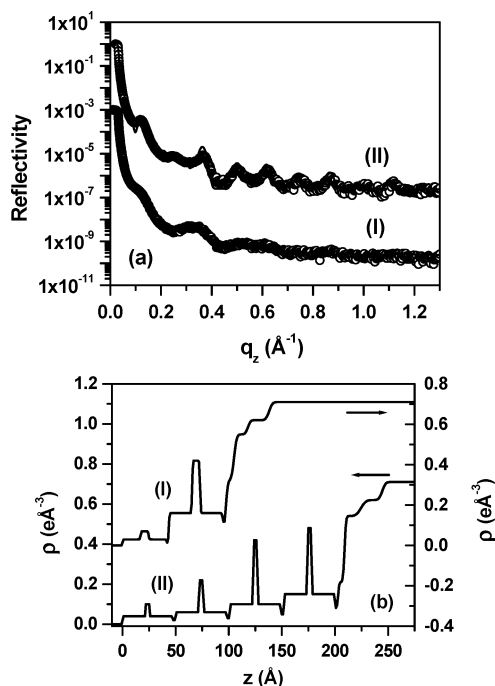


Figure 5. (a) X-ray reflectivity profiles (circles) and corresponding fitted curves (solid line) of the films of stearic acid in the presence of Pb ions in subphase water deposited (I) just after collapse and (II) far after collapse. (b) Average electron density (ρ) versus depth (z) extracted from the fit of reflectivity profiles I and II.

Ries mechanism. It is clear that the initial 3D nucleation centers formed in the fast nucleation region (region I) consist of trimolecular layers with a surprisingly high degree of coherence between the top and bottom of the 3D nucleation centers. In the second phase (region II) these nucleation centers fuse and grow to a multilayer. It is interesting to note that the greater loss of coherence

between the top and bottom surfaces of the collapsed film occurs when the surface pressure of this film starts to rise again, rather than in this second phase.

One of the important points to be noted from our study is that the metal ions which produce constant area collapse, viz., Cd and Pb, are also known to produce chiral distortion^{27,28} in the Langmuir monolayer whereas the metal ions which produce constant pressure collapse, in particular Mn, Mg, and Zn, do not produce any chiral distortion.^{22,27} It is also known that Pb ions, at normal subphase pH,²⁹ and Cd ions, at elevated subphase pH,³⁰ form metal–metal bonds in the presence of a Langmuir monolayer of fatty acids and these complexes are strongly attracted to the fatty acid headgroups, thereby condensing the monolayer quite considerably. The chiral distortion and condensation are consistent with metal–metal complex formation through an anisotropic polar bond with the headgroup. Hence, the monolayers in the presence of Pb ions and Cd ions (at higher subphase pH) are more rigidly bonded structures relative to the monolayers in the presence of Mg ions and Mn ions, where such chirality or metal–metal-bonded complexes have not been observed. When, at $\pi \geq \pi_c$, the monolayer starts to fold, the rigidity of the monolayer in the former case (i) causes this fold to grow to a considerable height and (ii) does not allow this fold to slip smoothly over the monolayer. These two effects lead to bending and breaking of the fold and to the formation of incoherent multilayers during constant area collapse. The fast growth of 3D nucleation centers that gives rise to the sudden reduction in π can also be explained if the nucleation centers are these large folds. The probable formation of cracks with Cd ions in the subphase indicates a more rigid monolayer than with Pb. Since Pb is more electronegative than Cd, the Cd–headgroup bond is not likely to be more polar (and hence stronger) than the Pb–headgroup bond. The source of this rigidity may then lie in a stronger Cd–Cd bond than a Pb–Pb bond, though we cannot furnish an explanation for this enhanced strength.

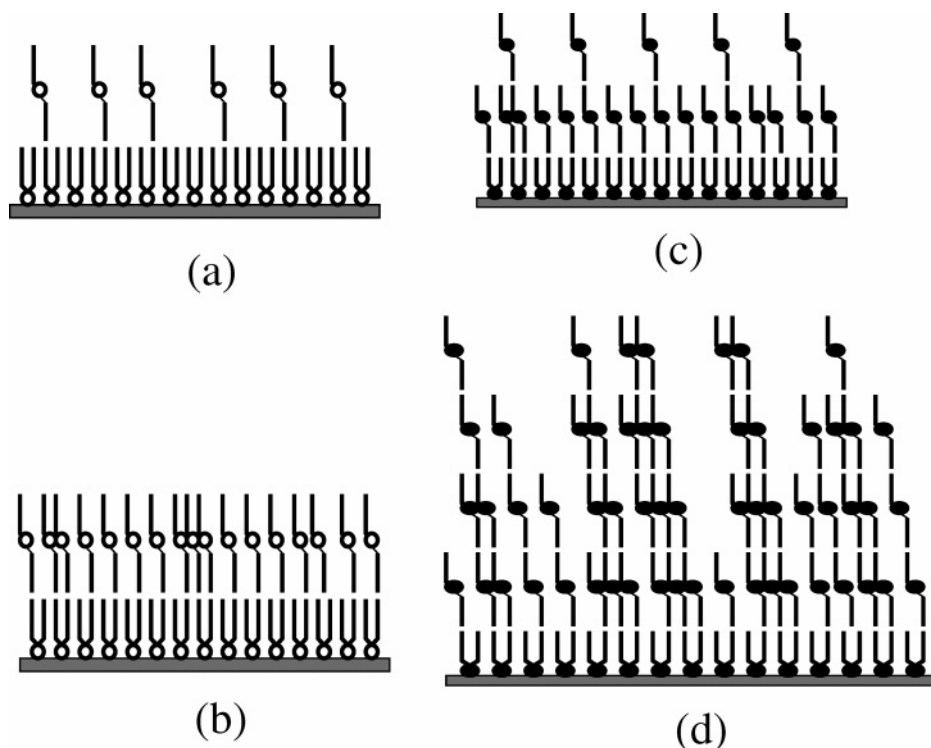


Figure 6. Cartoons depicting the deposited layered structures after collapse. Constant pressure collapse: (a) just after collapse and (b) far after collapse. Constant area collapse: (c) just after collapse and (d) far after collapse. Open circles denote headgroups bearing Mn and Co, whereas filled circles denote Cd- or Pb-bearing headgroups.

In the case of the Mg and Mn ions, polar bonds with headgroups or metal–metal bonds have not been detected or inferred, and the bonding with headgroups is presumably more electrovalent in character. When monolayers in the presence of such isotropic flexible bonds undergo folding, the folds easily slip over the monolayer and neither formation of large folds nor any incoherent process such as breaking takes place. The 3D nucleation center is then the bimolecular layer. These centers increase continuously in number as the monolayer is compressed.

It is to be noted that Zn and Cd occupy the same group in the periodic table but they behave very differently in the subphase in the presence of Langmuir monolayers, whereas Mg, Mn, Co, and Zn are in different groups but behave in quite similar ways, as also do Cd and Pb though, again, they are in different groups. Also, the role of water in mediating the interactions between ions and between

ions and headgroups has been found to be very important.^{28,29} A straightforward connection between electronic structure of metals and behavior of Langmuir monolayers with the hydrated ions of these metals seems quite difficult at this stage.

Conclusion

We have shown through π -A isotherm studies of collapsing Langmuir monolayers that the presence of metal ions which chirally distort the monolayers causes a constant area collapse, whereas the presence of metal ions that do not create chiral distortion causes a constant pressure collapse. We have also shown from X-ray reflectivity studies of collapsed monolayers transferred horizontally onto Si(001) using a modified inverted Langmuir–Schaefer method that there is a clear morphological distinction between monolayers undergoing constant pressure and constant area collapses. Whereas in the former only a coherent bimolecular layer is formed at all stages of collapse, in the latter first a coherent trimolecular layer is formed and then the number of molecular layers increases with the progress of collapse.

LA0505770

(27) Datta, A.; Kmetko, J.; Yu, C. J.; Richter, A. G.; Chung, K. S.; Bai, J. M.; Dutta, P. *J. Phys. Chem. B* **2000**, *104*, 5797.

(28) Kmetko, J.; Datta, A.; Evmenenko, G.; Durbin, M. K.; Richter, A. G.; Dutta, P. *Langmuir* **2001**, *17*, 4697.

(29) Boyanov, M. I.; Kmetko, J.; Shibata, T.; Datta, A.; Dutta, P.; Bunker, B. A. *J. Phys. Chem. B* **2003**, *107*, 9780.

(30) Kundu, S.; Datta, A.; Hazra, S. *Chem. Phys. Lett.* **2005**, *405*, 282.